

# Capture, thermalisation and annihilation of Dark Matter in Compact Objects

---

**Giorgio Busoni**<sup>a,\*</sup>

<sup>a</sup>ARC Centre of Excellence for Dark Matter Particle Physics,  
Department of Physics, University of Adelaide, Adelaide, SA 5005, Australia  
E-mail: [giorgio.busoni@adelaide.edu.au](mailto:giorgio.busoni@adelaide.edu.au)

We present an improved treatment of heavy dark matter scattering in white dwarfs, accounting for multiple collisions required for gravitational capture. Our analysis includes dark matter trajectories, nuclear form factors, and radial profiles for escape velocity and target densities. We find capture rates that differ significantly from previous estimates based on Earth-like approximations. Additionally, we compute the thermalisation timescale, incorporating in-medium effects such as phonon interactions in crystallized cores. Our results indicate much shorter thermalisation timescales than previously thought, emphasizing the importance of our approach in determining the cross section for accumulated asymmetric dark matter to self-gravitate.

*The XVIth Quark Confinement and the Hadron Spectrum Conference (QCHSC24)*  
19-24 August, 2024  
Cairns Convention Centre, Cairns, Queensland, Australia

---

\*Speaker

## 1. Introduction

White dwarfs (WDs) are the most common stellar remnants, comprising over 90% of stars in the Galaxy. Their high density and extreme conditions, combined with available observational data, make them valuable for testing dark matter (DM) models. In particular, DM accumulation in WDs can lead to observable effects such as increased luminosity [1] or DM-induced supernovae and black hole formation [2]. The latter requires capturing heavy DM particles  $\gtrsim O(100\text{ TeV})$ , which necessitates multiple collisions to lose enough energy and become gravitationally bound.

Existing analytical approaches for multi-scattering DM capture in stars [3, 4] are based on Gould’s formalism for Earth capture [5]. However, this framework assumes constant escape velocity and density, as well as linear DM trajectories, which hold in Earth’s weak gravitational field but break down in WDs. Given the much higher velocities DM reaches when falling into WDs—comparable to a significant fraction of the speed of light—these approximations can severely overestimate capture rates.

In this work, we develop a refined formalism for DM capture in WDs, properly accounting for nuclear form factors, varying escape velocity, and gravitational focusing. We first analyze DM scattering with a single WD constituent and then generalize to a multi-component ionic mixture. Our findings indicate that prior assumptions significantly overestimate capture rates, especially for heavier DM.

Once captured, DM continues scattering until thermal equilibrium is reached. Previous estimates of thermalisation times [6–8] were based on high-energy scattering, but we show that low-energy interactions, particularly in a crystallized WD core, play a key role. We incorporate finite-temperature effects and collective excitations in Coulomb lattices, finding that thermalisation times are significantly shorter than previously thought.

To highlight the impact of our improved approach, we apply it to the case of heavy, non-annihilating asymmetric DM. We determine the DM-nucleon cross section required for accumulated DM to self-gravitate, incorporating the evolving WD core temperature and thermalisation timescale. Depending on the WD’s composition and compactness, our results differ from previous estimates by at least an order of magnitude.

## 2. Capture rate by multiple scattering

### 2.1 Single scattering limit

We start by examining the scenario where a single collision with the non-relativistic, non-degenerate ions in the WD core is sufficient to gravitationally bind DM to the star. In this situation, the most general form for the DM capture rate  $C_1$  is given by [9]

$$C_1 = \frac{\rho_\chi}{m_\chi} \int_0^\infty du_\chi \frac{f_{\text{MB}}(u_\chi)}{u_\chi} \int_0^{R_\star} dr 4\pi r^2 n_T(r) v_{\text{esc}}^2(r) \sigma_{T\chi}(v_{\text{esc}}(r)) \eta(r). \quad (1)$$

where  $\rho_\chi$  and  $m_\chi$  represent the local DM density and DM mass,  $f_{\text{MB}}(u_\chi)$  corresponds to the DM speed distribution in the star’s frame, assumed to follow a Maxwell-Boltzmann distribution,  $n_T(r)$  is the target ion number density, and  $v_{\text{esc}}(r)$  denotes the escape velocity from the star at a distance

$r$  from its center, the factor  $\eta$  accounts for the star opacity,

$$\eta(r) = \frac{1}{2} \int_0^1 \frac{y dy}{\sqrt{1-y^2}} \left( e^{-\tau_-(r,y)} + e^{-\tau_+(r,y)} \right). \quad (2)$$

with  $\tau_\chi^\pm(r, y)$  are the optical depths of the 2 possible trajectories, and

$$\sigma_{T\chi} = \int_{E_R^{\min}}^{E_R^{\max}} dE_R \frac{d\sigma_{T\chi}}{dE_R}(v_{\text{esc}}, E_R), \quad (3)$$

where  $E_R^{\max}$  and  $E_R^{\min}$  are the maximum kinematic energy of the scattering and the minimum energy needed for capture, respectively. For sufficiently light DM, the minimum energy can be approximated as zero.

## 2.2 Multiple Scattering and Response Function

When the DM is heavy enough, Eq. 1 would underestimate the correct result, because in this case, DM requires multiple collisions to become gravitationally bound to the star. To address this, we construct a function that encapsulates both the non-linear effects of stellar opacity and multiple interactions with ionic targets.

We first define a probability density function for the energy lost by a DM particle during a collision:

$$f(E_R) = \frac{1}{\sigma_{T\chi}} \frac{d\sigma_{T\chi}}{dE_R}(E_R). \quad (4)$$

The probability that DM loses an energy of at least  $\delta E = m_\chi u_\chi^2/2$  from a single collision is given by

$$\mathcal{F}_1(\delta E) = \int_{\delta E}^{\infty} dE_R f(E_R), \quad (5)$$

where the upper limit of integration is extended to infinity, which is valid due to the high escape velocity in white dwarfs. Similarly, the probability that DM loses the same amount of energy after  $N$  scatterings is given by

$$\mathcal{F}_N(\delta E) = \int_0^{\delta E} dE_R \mathcal{F}_{N-1}(\delta E - E_R) f(E_R). \quad (6)$$

Assuming for simplicity that the DM-target cross section is well approximated by

$$\frac{d\sigma_{T\chi}}{d \cos \theta_{\text{cm}}} \propto e^{-\frac{E_R}{E_0}}, \quad (7)$$

where  $E_R$  is the energy lost in the recoil and  $E_0$  depends on the nuclear target, and using exponential nuclear form factors similar to the Helm approximation, we obtain

$$f(E_R) = \frac{\Theta(E_R)}{E_0} e^{-\frac{E_R}{E_0}}, \quad \mathcal{F}_1(\delta E) = e^{-\frac{\delta E}{E_0}}. \quad (8)$$

By defining the dimensionless parameter  $\delta = \frac{\delta E}{E_0} = \frac{m_\chi u_\chi^2}{2E_0}$  and taking the Laplace transform of the  $\mathcal{F}$  functions, we find

$$\tilde{\mathcal{F}}_1(s) = \frac{1}{1+s}, \quad \tilde{\mathcal{F}}_N(s) = \frac{1}{(1+s)^N}, \quad \mathcal{F}_N(\delta) = \frac{e^{-\delta} \delta^{N-1}}{N-1!}. \quad (9)$$

To account for multiple scatterings, we use the Poisson distribution [5] for the probability of  $N$  collisions:

$$p_N(\tau_\chi) = e^{-\tau_\chi} \frac{\tau_\chi^N}{N!}. \quad (10)$$

where  $\tau_\chi$  represents the optical depth of the DM path length. Substituting  $\mathcal{F}_1(\delta)$  and  $p_0$  into Eq. 1 and 3, we rewrite the single scattering result as

$$C_1 = \frac{\rho_\chi}{m_\chi} \int_0^{R_\star} dr 4\pi r^2 n_T(r) \sigma_{T\chi}(v_{\text{esc}}(r)) v_{\text{esc}}^2(r) \int_0^1 \frac{y dy}{\sqrt{1-y^2}} \int_0^\infty du_\chi \frac{f_{\text{MB}}(u_\chi)}{u_\chi} p_0(\tau_\chi) \mathcal{F}_1(\delta). \quad (11)$$

With the above definitions, it is trivial to now generalize the above equation to  $N$  scatterings as

$$C_N = \frac{\rho_\chi}{m_\chi} \int_0^{R_\star} dr 4\pi r^2 n_T(r) \sigma_{T\chi}(v_{\text{esc}}(r)) v_{\text{esc}}^2(r) \int_0^1 \frac{y dy}{\sqrt{1-y^2}} \int_0^\infty du_\chi \frac{f_{\text{MB}}(u_\chi)}{u_\chi} p_{N-1}(\tau_\chi) \mathcal{F}_N(\delta). \quad (12)$$

The total capture rate is given by the sum over all  $N$  collisions,  $C = \sum_N C_N$ . Now, we sum the series first, obtaining the response function,  $G(\tau_\chi, \delta)$

$$G(\tau_\chi, \delta) \equiv \sum_{N=1}^\infty p_{N-1}(\tau_\chi) \mathcal{F}_N(\delta) = \sum_{N=1}^\infty \frac{e^{-\tau_\chi} \tau_\chi^{N-1}}{(N-1)!} \frac{e^{-\delta} \delta^{N-1}}{(N-1)!} = e^{-\tau_\chi - \delta} I_0(2\sqrt{\tau_\chi \delta}), \quad (13)$$

where  $I_0$  is the modified Bessel function of the first kind  $I_n$  for  $n = 0$ . This function describes the probability that a DM particle loses at least  $\delta E$  through multiple scatterings, after traversing a medium with an optical depth  $\tau_\chi$ .

The function  $G$  needs to be averaged over the two possible optical depths and all values of angular momentum, as done with  $\eta$ . This leads to

$$\tilde{G}(r, \delta) = \int_0^1 dy \frac{y dy}{\sqrt{1-y^2}} \frac{G(\tau_\chi^-(r, y), \delta) + G(\tau_\chi^+(r, y), \delta)}{2}. \quad (14)$$

The final expression for the total capture rate reads

$$C = \frac{\rho_\chi}{m_\chi} \int_0^{R_\star} dr 4\pi r^2 n_T(r) v_{\text{esc}}^2(r) \sigma_{T\chi}(v_{\text{esc}}(r)) \int_0^\infty du_\chi \frac{f_{\text{MB}}(u_\chi)}{u_\chi} \tilde{G}\left(r, \frac{m_\chi u_\chi^2}{2E_0}\right). \quad (15)$$

Fig. 1 compares our refined approach (magenta) with earlier methods by ref. [3] (light blue) and ref. [4] (orange). For scalar-scalar interactions and DM masses of  $10^3$  GeV and  $10^6$  GeV, for a  $1M_\odot$  WD made of carbon, located in the solar neighborhood, i.e., we assume  $\rho_\chi = 0.4$  GeV/cm<sup>3</sup>,  $v_\star = 220$  km/s and  $v_d = 270$  km/s. We plot the results as the fraction of the maximal capture rate that can be achieved, the geometric limit, which is

$$C_{\text{geom}} = \frac{\pi R_\star^2 \rho_\chi}{m_\chi} \int_0^\infty \frac{w^2(R_\star)}{u_\chi} f_{\text{MB}}(u_\chi) du_\chi, \quad (16)$$

$$= \frac{\pi R_\star^2 \rho_\chi}{3v_\star m_\chi} \left[ (3v_{\text{esc}}^2(R_\star) + 3v_\star^2 + v_d^2) \text{Erf}\left(\sqrt{\frac{3}{2}} \frac{v_\star}{v_d}\right) + \sqrt{\frac{6}{\pi}} v_\star v_d e^{-\frac{3v_\star^2}{2v_d^2}} \right]. \quad (17)$$

The results show that:

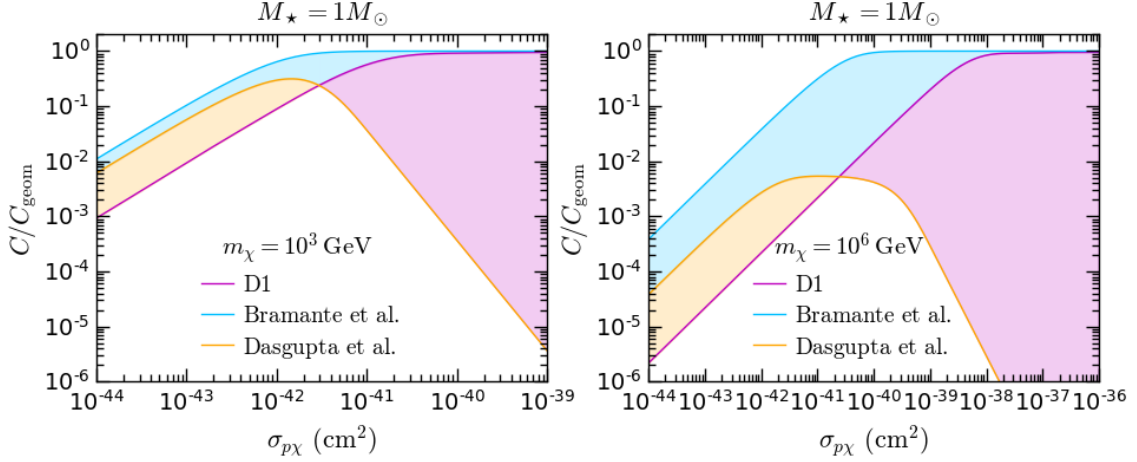


Figure 1: Capture rate in the multiple scattering regime (magenta) for a  $1M_{\odot}$  WD made of carbon, considering scalar-scalar interactions (D1) and  $m_{\chi} = 10^3$  GeV and  $10^6$  GeV. We also show results obtained using the prescriptions in refs. [3] (light blue) and [4] (orange).

- **Overestimation by Simplified Models:** Approximations that neglect the full radial dependence of escape velocity, target density, and form factors overestimate the capture rate by at least one order of magnitude for DM-nucleon cross-sections  $\sigma_{p\chi} \lesssim 10^{-42} \text{ cm}^2$ .
- **Form Factor Assumptions:** Previous works assumed that the nuclear form factor saturates to  $\sim 0.3$  [4] or  $0.5$  [3], while the full calculation shows saturation at approximately  $\sim 0.034$  for the scalar-scalar operator and low recoil energies.
- **Truncation Effects:** the approach of ref. [4] fails to reach the geometric limit for large cross-sections due to the truncation of the sum over collisions at a maximum value.
- **Motion of the WD:** ref. [3] neglects the motion of the WD, causing an overestimation of both the capture rate and the threshold cross-section at which the geometric limit is achieved.

### 3. Thermalisation

The process of thermalisation can be categorized into two main phases. The initial phase occurs when the orbit of the captured DM extends beyond the boundaries of the star. The subsequent phase begins once the DM's orbit is completely enclosed within the star and concludes when thermal equilibrium is established at the center of the WD. This first phase typically progresses much faster than the second, contributing less than 1% to the overall thermalisation duration [6]. For this reason, our analysis concentrates on the second phase to estimate the thermalisation timescale.

During the latter phase, two distinct kinematic regimes emerge based on whether the DM velocity or the target velocity primarily determines the relative velocity of their interactions. The core of a WD is assumed to be relatively uniform in both temperature and density. Since the majority of the thermalisation time occurs in the second kinematic regime, where the DM energy is low, it is reasonable to evaluate interaction rates within the central region of the WD.

To calculate the thermalisation time, we employ the temperature-dependent differential interaction rate, which incorporates the thermal motion of the nuclei.

To derive analytic expressions for the thermalisation time, we take the limit of large number of scatterings, approximating the energy loss as continuous rather than discrete process [10]

$$\frac{dx}{dt} = E(x), \quad (18)$$

$$t_{\text{therm}} = \int_1^\infty \frac{dx}{E(x)}, \quad (19)$$

$$E(x) = \int_0^x dy (x-y) R^-(x \rightarrow y), \quad (20)$$

where we assume the initial energy is infinitely large, as the DM energy upon capture is considerably greater than its energy at thermal equilibrium. This approximation becomes increasingly accurate for smaller fractional energy losses, as a greater number of scatterings is needed to thermalize the DM. Specifically, at low energies, the mean energy transfer is approximately  $\langle \Delta x \rangle \approx O(1) \times \sqrt{x/\mu}$ , while at high energies,  $\langle \Delta x \rangle \approx 2x/\mu$ . Both approximations hold more precisely for large DM masses.

Additionally, we disregard the up-scattering rate. While up-scattering is negligible at higher energies, it may have a modest effect near thermalisation, altering the result by an  $O(1)$  factor. Therefore, the thermalisation time calculations presented here should be interpreted as order-of-magnitude estimates.

For simplicity, we also omit the influence of nuclear form factors on the thermalisation time. This is justified because the exponential suppression from form factors becomes significant only for energy losses exceeding  $\langle \Delta K_\chi \rangle \sim 2K_\chi/\mu \gtrsim E_0 \approx O(\text{MeV})$ , while the thermalisation time is primarily driven by scatterings at lower energies, where form factors have a minimal impact.

Eq. 20 can be computed analytically in two limiting cases: when  $K_\chi \gg T_\star$  (high energy) and when  $K_\chi \sim T_\star$  (low energy), corresponding to  $x \gg 1$  and  $x \sim 1$ , respectively.

In the regime of large energy transfers ( $x \gg 1$ ), the expression for  $E(x)$  takes the form

$$E(x) \simeq \begin{cases} 2n_T(r)\sigma_T \left(\frac{x}{\mu}\right)^{m+3/2} v_T^{2m+1}, & d\sigma_{T\chi} \propto v_{\text{rel}}^{2m} \\ \frac{4(m+1)}{m+2} n_T(r)\sigma_T v_T \left(\frac{x}{\mu}\right)^{m+3/2} \left(\frac{2m_T^2 v_T^2}{q_0^2}\right)^m, & d\sigma_{T\chi} \propto q_{\text{tr}}^{2m} \end{cases} \quad (21)$$

In the low energy regime, i.e.  $x \sim 1$  we find  $v_{\text{rel}}^{2m}$

$$E(x) \sim \begin{cases} \Gamma\left(m + \frac{3}{2}\right) \frac{n_T(r)\sigma_T}{\sqrt{\pi}} \sqrt{\frac{x}{\mu}} v_T^{2m+1}, & d\sigma_{T\chi} \propto v_{\text{rel}}^{2m} \\ \Gamma\left(m + \frac{3}{2}\right) \frac{2(m+1)}{m+2} \frac{n_T(r)\sigma_T v_T}{\sqrt{\pi}} \sqrt{\frac{x}{\mu}} \left(\frac{2m_T^2 v_T^2}{q_0^2}\right)^m, & d\sigma_{T\chi} \propto q_{\text{tr}}^{2m} \end{cases} \quad (22)$$

From these expressions, we can note that it is important to use the right kinematic regime ( $x \sim 1$ ) to compute the thermalisation time, as this leads to a very different scaling in  $x$  and  $\mu$ . The resulting

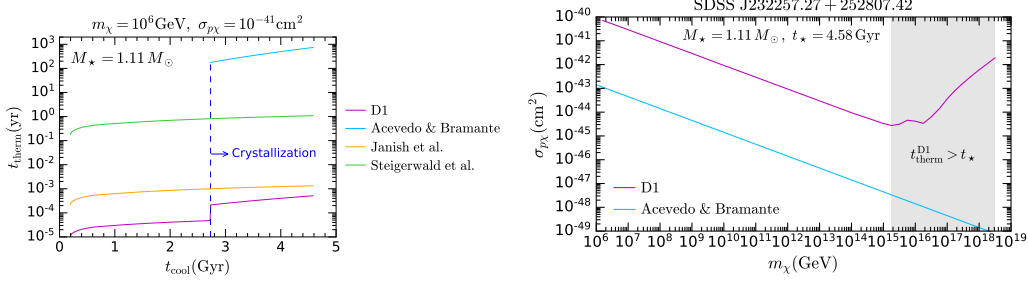


Figure 2: Left: thermalisation time as a function of the WD cooling age for the WD SDSS J232257.27+252807.42 ( $M_\star = 1.11 M_\odot$ ), DM of mass  $m_\chi = 10^6$  GeV, and a DM-proton scalar-scalar cross section of  $\sigma_{p\chi} = 10^{-41} \text{ cm}^2$ . Our result is depicted in magenta, ref. [6] is shown in light blue, while results using the corresponding prescriptions from refs. [7] and [8] are depicted in orange and green, respectively. The dashed blue line represents the onset of crystallisation. Right: DM-proton cross section required to reach the self-gravitation condition, assuming scalar-scalar interactions (D1, in magenta). For comparison we show in light blue results obtained used the condition given in ref. [6].

thermalisation times are

$$t_{\text{therm}} \propto \begin{cases} \frac{\mu}{n_T^c \sigma_T v_T} \frac{1}{v_T^{2m}}, & d\sigma_{T\chi} \propto v_{\text{rel}}^{2m} \\ \frac{\mu}{n_T^c \sigma_T v_T} \left( \frac{q_0^2}{2v_T^2 m_T^2} \right)^m, & d\sigma_{T\chi} \propto q_{\text{tr}}^{2m} \end{cases} \quad (23)$$

Fig. 2 illustrates the variation of the thermalisation timescale across the evolution (cooling time  $t_{\text{cool}}$ ) of the  $1.11 M_\odot$  WD SDSS J232257.27+252807.42 (left), and the corresponding upper bound on the DM cross section derived from the fact that he hasn't collapsed (right). We consider the scalar-scalar operator (D1), DM of mass  $m_\chi = 10^6$  GeV and a DM-proton cross section of  $\sigma_{p\chi} = 10^{-41} \text{ cm}^2$ . We include the effects arising from the fact that the core of the WD begins solidifying (at  $t_{\text{cool}} < 2.73$  Gyr for this particular WD). Note the sudden increase in the thermalisation time (magenta line) once the crystallisation front starts moving from the WD center onwards. For comparison, we also show in Fig. 2 results using other prescriptions in the literature.

#### 4. Conclusions

In this work, we have revisited the calculation of the capture rate for heavy dark matter (DM) in white dwarfs (WDs). For DM in this mass range, multiple collisions are needed for it to become gravitationally bound to the star. We extended the formalism from the single-scattering to the multiple-scattering regime by introducing a response function that encapsulates the cumulative probability for DM to lose at least an energy  $\delta E$  through repeated collisions.

Our approach includes gravitational focusing, nuclear form factors, variations in the escape velocity within the WD, and the DM-target relative velocity. We demonstrated that incorporating these often-overlooked effects modifies the capture rate by several orders of magnitude, with the



impact being particularly significant for very heavy DM. The response function method accommodates DM-nucleon interactions that are momentum or velocity suppressed and can be extended to account for DM capture through interactions with multiple targets.

After being captured, DM continues to scatter within the star, gradually losing energy until it settles at the core and reaches thermal equilibrium. We estimated the thermalisation time for both non-crystallized and crystallized cores. In the latter case, in-medium effects like phonon emission and absorption slow down the process due to the low-momentum transfers involved in the final stages. However, we find that this delay increases the thermalisation time by less than an order of magnitude—a significantly smaller effect than previously estimated.

Finally, to emphasize the importance of accurately calculating the multi-scattering capture rate and thermalisation time, we applied our framework to non-annihilating DM accumulated in a WD core over its lifetime. Our results show that the DM-nucleon cross sections required for accumulated DM to become self-gravitating are corrected by several orders of magnitude.

## References

- [1] G. Bertone and M. Fairbairn, “*Compact Stars as Dark Matter Probes*,” *Phys. Rev. D* **77** (2008) 043515, [arXiv:0709.1485 \[astro-ph\]](#).
- [2] P. W. Graham, S. Rajendran, and J. Varela, “*Dark Matter Triggers of Supernovae*,” *Phys. Rev. D* **92** no. 6, (2015) 063007, [arXiv:1505.04444 \[hep-ph\]](#).
- [3] J. Bramante, A. Delgado, and A. Martin, “*Multiscatter stellar capture of dark matter*,” *Phys. Rev. D* **96** no. 6, (2017) 063002, [arXiv:1703.04043 \[hep-ph\]](#).
- [4] B. Dasgupta, A. Gupta, and A. Ray, “*Dark matter capture in celestial objects: Improved treatment of multiple scattering and updated constraints from white dwarfs*,” *JCAP* **08** (2019) 018, [arXiv:1906.04204 \[hep-ph\]](#).
- [5] A. Gould, “*Big bang archeology: WIMP capture by the earth at finite optical depth*,” *Astrophys. J.* **387** (1992) 21.
- [6] J. F. Acevedo and J. Bramante, “*Supernovae Sparked By Dark Matter in White Dwarfs*,” *Phys. Rev. D* **100** no. 4, (2019) 043020, [arXiv:1904.11993 \[hep-ph\]](#).
- [7] R. Janish, V. Narayan, and P. Riggins, “*Type Ia supernovae from dark matter core collapse*,” *Phys. Rev. D* **100** no. 3, (2019) 035008, [arXiv:1905.00395 \[hep-ph\]](#).
- [8] H. Steigerwald, V. Marra, and S. Profumo, “*Revisiting constraints on asymmetric dark matter from collapse in white dwarf stars*,” *Phys. Rev. D* **105** no. 8, (2022) 083507, [arXiv:2203.09054 \[astro-ph.CO\]](#).
- [9] N. F. Bell, G. Busoni, S. Robles, and M. Virgato, “*Heavy dark matter in white dwarfs: multiple-scattering capture and thermalization*,” *JCAP* **07** (2024) 051, [arXiv:2404.16272 \[hep-ph\]](#).
- [10] B. Bertoni, A. E. Nelson, and S. Reddy, “*Dark Matter Thermalization in Neutron Stars*,” *Phys. Rev. D* **88** (2013) 123505, [arXiv:1309.1721 \[hep-ph\]](#).